Heliyon 10 (2024) e23533

Contents lists available at ScienceDirect

Heliyon

journal homepage: www.cell.com/heliyon

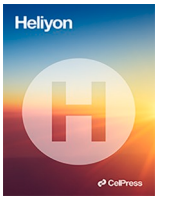

An exploration of the effect of Chinese herbal compound on the occurrence and development of large intestine cancer and intestinal flora

Pingyu Liu [a,1], Jian Ying [b,1], Xin Guo [a], Xiaohui Tang [b], Wenjuan Zou [b], Tiantian Wang [c], Xinyi Xu [a], Bin Zhao [b], Na Song [b,**], Jun Cheng [b,*]

[a] Hunan University of Chinese Medicine, Changsha, 410208, Hunan, China
[b] Department of Oncology, Chongqing Hospital of Traditional Chinese Medicine, Chongqing, 400021, China
[c] Department of Emergency Intensive Care, Chongqing Hospital of Traditional Chinese Medicine, Chongqing, 400021, China

ARTICLE INFO

Keywords:
Chinese herbal compound
Large intestine cancer
AOM/DSS-Induced colorectal cancer mice
16S rRNA
Inflammation

ABSTRACT

This study was conducted to observe the effect of Chinese herbal compound on the treatment of colon cancer using AOM/DSS-induced C57BL/6J colon cancer mice and to validate potential influence on intestinal flora of mice. A colorectal cancer (CRC) mouse model was built with a total of 50 C57BL/6J mice that were induced by administrating AOM/DSS. These experimental animals were split up into 5 groups, a control group, a model group, and low-, medium- and high-dose Chinese herbal compound groups. All mice were given Chinese herbal compound treatment, and the colon tissues of each group were harvested with the length measured and the number of colon polyps accounted. The Ki-67 expression in the colon tissues was detected via immunohistochemistry. Relative quantification of the expression of genes and proteins was determined through qPCR and WB assays. Contents of IL-6, TNF-α, IFN-γ, and IL-10 in serum and colon tissues of mice were determined by ELISA. An additional 16S rRNA sequencing analysis was implemented for the identification of mouse intestinal flora. The results suggested that all low-, medium- or high-dose Chinese herbal compound could markedly inhibit the shortening of colon length and significant number reduction of colon polyps in the model group. The relative expression of genes and proteins (PCNA, Muc16, and MMP-9) associated with proliferation in mouse colon tissues were inhibited. In addition, compared with the model group, the contents of IL-6, TNF-α, and IFN-γ in serum and colon tissues were substantially decreased in the high-dose Chinese herbal compound group, thereby reducing the structure damage in colon tissues and the infiltration degree of inflammatory cells. Besides, the expression of TLR4/MyD88/NF-κB protein was markedly decreased. The 16S rRNA sequencing analysis demonstrated that mice in the model group had decreased intestinal flora diversity, and there were significant changes in flora abundance and amino acid metabolism between the control group and the model group. Taken together, the treatment of Chinese herbal compound against CRC in this study might be regulated

* Corresponding author. Department of Oncology, Chongqing Hospital of Traditional ChineseMedicine, No.6, Panxi Qi Zhi Road, Jiangbei District, Chongqing, 400021, China.
** Corresponding author. Department of Oncology, Chongqing Hospital of Traditional Chinese Medicine, No.6, Panxi Qi Zhi Road, Jiangbei District, Chongqing, 400021, China.
E-mail addresses: songna896600@163.com (N. Song), 13206075951@163.com (J. Cheng).
[1] Pingyu Liu and Jian Ying contributed equally.

https://doi.org/10.1016/j.heliyon.2023.e23533
Received 30 May 2023; Received in revised form 5 December 2023; Accepted 5 December 2023
Available online 10 December 2023

by the TLR4/MyD88/NF-κB signaling pathway, and the imbalance in intestinal flora was also closely related to CRC occurrence.

1. Introduction

Large intestine cancer includes colon cancer and rectal cancer, which is a kind of malignant tumor in digestive system with high incidence and high mortality. According to statistics, there are 1.8 million new cases of colorectal cancer (CRC) and 860,000 deaths every year, ranking third in the incidence of malignant tumors and second in the mortality rate in the world [1]. The incidence of CRC in China has increased recently and malignant tumor incidence and mortality rank CRC second in incidence and fourth in mortality based on the statistics in 2020 [2]. When it comes to CRC, surgery is still the preferred treatment currently. However, with the popularization of traditional Chinese medicine, its application in tumor treatment has also been paid attention [3], and the role of traditional Chinese medicine in the prevention and treatment of CRC has been recognized [4,5].

Several factors contribute to the occurrence and development of large intestine cancer, including heredity, environment, and lifestyle [6–8]. While early surgical intervention and postoperative chemotherapy have demonstrated effectiveness in managing CRC, there remain considerable hurdles in its treatment, including postoperative complications, elevated recurrence and metastasis rates, drug resistance, and the potential for medication-related side effects [9,10]. Traditional Chinese medicine (TCM) is involved in the modern clinical treatment of large intestine cancer by integrating traditional Chinese and western medicine, which includes TCM-assisted chemotherapy, radiotherapy, and other therapeutic means [11]. These methods have the potential to enhance treatment efficacy, minimize adverse reactions, exert a multi-faceted anti-colorectal cancer effect through various targets and pathways, and prolong the survival of patients [12]. Furthermore, substantial clinical evidence substantiates the effectiveness of traditional Chinese medicine and its components in inhibiting the proliferation of colorectal cancer cells, inducing apoptosis, arresting the cell cycle, promoting autophagy, and suppressing angiogenesis as part of their anti-colorectal cancer mechanisms [13–16].

The intestinal microbiota is a crucial element of symbiotic microorganisms within the host organism, capable of influencing tumor development by modulating the tumor microenvironment and biofilm formation. It is intricately linked to the onset, advancement, and treatment of colorectal cancer [17,18]. Other studies have also shown that intestinal microorganisms participate in bile acid metabolism, amino acid metabolism, and short-chain fatty acid metabolism, which are also believed to be related to the occurrence of CRC [19]. Toll-like receptor 4 (TLR4) is a receptor primarily located on the surface of immune cells [20]. It functions as a pattern recognition receptor capable of identifying PAMPs, which encompass external TLR4 agonists like bacteria, viruses, fungi, and lipopolysaccharides (LPS) [21]. The interaction between Toll-like receptor 4 (TLR4) and adaptor molecule Myeloid differentiation primary response gene 88 (MyD88) is crucial for activating downstream signaling pathways and inducing inflammatory responses [22]. Nuclear factor-kappa B (NF-κB) is a transcription factor involved in the regulation of various genes, including inflammatory factors and apoptosis-related factors [23]. Activation of the TLR4/MyD88 signaling pathway triggers NF-κB activation, thereby promoting tumor growth and development [24]. The study by Bi et al. [25] indicated that Fusobacterium nucleatum can significantly upregulate the expression of miR-21 through the TLR4/MYD88/NF-κB pathway, promoting the progression of colitis-associated colorectal cancer. Sun et al. [26] reported that targeting BMI1 as an anti-inflammatory target can regulate the invasion and epithelial-to-mesenchymal transition (EMT) of colorectal cancer cells through the TLR4/MD-2 MyD88 complex-mediated NF-κB signaling pathway.

In this paper, we believed that exploring the mechanisms of CRC-related signaling pathways can help us better identify potential anti-CRC targets for traditional Chinese medicine. Furthermore, an examination of the mechanisms by which intestinal flora induces CRC and the ability of TCM to prevent and treat CRC by regulating intestinal flora will provide valuable insights for the prevention and treatment of colorectal cancer via traditional Chinese medicine. Contextually, the effect of the Chinese herbal compound on the TLR4/MyD88/NF-κB pathway was investigated in vivo. The effects of Chinese herbal compounds on the intestinal flora of mice with large intestine cancer were investigated by 16S rRNA sequencing. These findings elaborated the mechanism of action of Chinese herbal compounds in the treatment of large intestine cancer and provided a new experimental basis for the clinical application of Chinese herbal compounds.

2. Materials and methods

2.1. Preparation of the Chinese herbal compound

This Chinese herbal compound contains 11 herbal ingredients including *Radix Astragali preparata* 30 g, *Pseudostellaria heterophylla (Miq.) Pax ex Pax et Hoffm*. 15 g, *Citrus reticulata Blanco* 15 g, sauteed *Atractylodes macrocephala Koidz*. 15 g, *Dioscorea opposita Thunb*. 15 g, *Euryale ferox Salisb*. 30 g, *Actinidia arguta (Sieb. & Zucc) Planch. ex Miq*. 30 g, *Scutellaria barbata D.Don* 30 g, *Ranunculus ternatus Thunb.* 15 g, *Hedyotis diffusa Willd* 30 g and *Salvia chinensis Benth.* 15 g. After placing the above Chinese herbs into the pot and soaking them in water for 30 min, they were boiled on high heat and then simmered on low heat for 15 min. Each batch of Chinese herbal formula ingredients was decocted twice, with 200 mL each time. After decoction, it was filtered and further processed into a medication solution with a dosage of 3.2 g/mL, serving as a reserve for high-dose Chinese herbal formula. The medium and low-dose medications were prepared by diluting with an equal amount of deionized water in a ratio of 6:3:1 for high, medium, and low doses respectively. The final concentrations of the medium and low-dose medications were 1.6 g/mL and 0.53 g/mL, respectively.

2.2. Establishment of AOM/DSS-induced CRC mouse model

An AOM/DSS-induced CRC mouse model was built with 6-week-old SPF male C57BL/6J mice, and a total of 50 animals were provided by Chongqing Ensiweier Biotechnology Co. LTD. All mice were fed in SPF-grade animal houses with alternating 12-h light-dark cycles. During the experiment, the mice had free access to food and water, and the temperature was controlled at 23–25 °C for adaptive feeding. They were randomly divided into 5 groups: Control, Model, Low dose herbal compound (L-Herbal compound), Medium dose herbal compound (M-Herbal compound), High dose Herbal compound (H-Herbal compound). Each group had 10 mice.

CRC model was induced in both model group and drug treatment group through AOM/DSS: each mouse in those groups received a daily intraperitoneal injection of AOM (approximately 0.1 mL) (Jinpin Chemical Technology (Shanghai) Co., LTD.) dissolved in normal saline at a dose of 10 mg/kg for 7 consecutive days. Starting from day 8, each mouse was provided with drinking water containing 3 % DSS (changed every three days) for 7 days. After that, the mice were fed with normal drinking water for 14 days. This 3 % DSS (Jinpin Chemical Technology (Shanghai) Co., LTD.) treatment cycle was repeated twice. In control group, mice received intraperitoneal injections of saline only on day 1 without DSS treatment. In drug treatment group, starting from the first day of modeling, mice were orally administered varying doses of the herbal compound (Low: 0.1 mL, Medium: 0.3 mL, High: 0.6 mL) until the end of the modeling period. In control and model groups, each mouse received 0.3 mL of PBS orally daily. The mice's body weight was measured every 10 d. Finally, after a 24-h fasting period, colonic tissues and serum samples were collected for subsequent research analysis.

2.3. Measurement of mouse colon length and HE staining of the pathological tissue sections

After the mice were sacrificed, colon tissues were taken, their length was measured and photographed, washed with PBS buffer solution, and fixed in 4 % paraformaldehyde solution. Paraffin sections (Thermo, FINESSE E+) were prepared by conventional means, and these sections were stained by HE according to the steps. First, the sample is washed with PBS and fixed. Dehydration process involved immersing the sample in ethanol multiple times, followed by transparency treatment using xylene. Subsequently, the tissue was soaked in molten paraffin for 2 h, and then it was embedded, sliced, and baked. The next step involved the dewaxing and rehydration of the paraffin sections, which were immersed under different conditions for 5–10 min. After that, HE staining was performed, which included staining with hematoxylin and eosin, as well as decolorization using a 1 % hydrochloric acid alcohol solution. Finally, the sections were dehydrated and sealed by immersing them in ethanol and xylene, respectively, and neutral resin was used for sealing. Upon microscopic examination, the results revealed blue nuclei and red or pink cytoplasm. Those necessary reagents were procured from Beijing Zhongshan Jinqiao Biotechnology Co., LTD. All HE-stained sections were examined under an optical microscope (Olympus, Thermo Scientific, USAIX50).

2.4. The ELISA detection of mouse serum

ELISA detection in this section was implemented for the contents of IL-6, TNF-α, IFN-γ, and IL-10 in mouse serum and colon tissues. IL-6, TNF-α, ELISA kit (Wuhan Yunclone Technology Co., LTD., batch No.: L211201967, L211201951); IFN-γ (# 430807) and IL-10 (#431411) ELISA kits were purchased from BioLegend. After blood collection, mice were placed at room temperature for 2 h, at 4 °C for 2 h until blood coagulation, centrifuged at 3000 r/min at 4 °C for 10 min, the supernatant was taken, centrifuged again once, serum was separated and then packed. Colon tissue homogenate was prepared and centrifuged at 13000 r/min at 4 °C for 30 min, then the supernatant was taken. The levels of IL-6, TNF-α, IFN-γ, and IL-10 in serum and colon of mice in each group were detected by ELISA according to the kit instructions.

2.5. Immunohistochemical assay for the positive expression of Ki-67 in colon tissue

The obtained tissues were embedded in paraffin wax, from which 4 μm slices were prepared to evaluate the Ki-67 expression. The colon tissues of each group were stained through immunohistochemistry assays according to kit instructions (Abcam: ab15580). Also, color development was performed with the DAB color development kit (Zhongshan Jinqiao, ZLI-9019), while redying was accomplished with the hematoxylin (Xavier, G1004). The prepared samples were separated by alcohol hydrochloride. The chromogenic site of Ki67 was the nucleus, and all the brown-yellow particles were positive cells. Optical microscopy was used to determine the expression of Ki67 in tumor tissues.

2.6. The mRNA detection of colon tissue

RNAiso Plus reagent (Takara, 9108) homogenate containing 50 mg colon tissue was added to 1 mL of pre-cooled homogenate. After 5 min at room temperature, the homogenate was centrifuged. The supernatant was absorbed from the prepared solution, in which chloroform of 1/5 volume of RNAiso Plus reagent was added, shaken and mixed for 15 s, left at room temperature for 5 min, and centrifuged for 15 min. The supernatant of the last prepared solution was retained, and isopropyl alcohol of equal volume was added into the solution, which was thoroughly mixed and then left for 10 min at 15–30 °C and centrifuged for 10 min. Then the supernatant was discarded, and 1 mL of 75 % ethanol was added into the test tube. The wall of the centrifuge tube was washed, and the ethanol was discarded after 5 min centrifugation. The obtained precipitation was dried for 4 min at room temperature, and then an appropriate amount of RNase-free water was added to dissolve the precipitation in the test tube, and stored in an ultra-low temperature refrigerator

at −80 °C. The centrifugal conditions were at 4 °C 12,000 rpm.

Colon tissue gene expression was analyzed with the TSE002 [2xT5 Fast qPCR Mix (SYBR Green I), Tsingke] as a reference. In the experiment of fluorescence quantitative PCR analysis, GAP-DH gene was deemed as the internal reference gene for fluorescence quantification of gene expression, and the primer sequences are shown in Table 1. The synthetic cDNA was taken as the template and was operated according to the instructions of the 2 × T5 Fast qPCR Mix (SYBR Green I) kit. The reaction system was built with the 2 × T5 Fast qPCR Mix (SYBR Green I) 10 μL, upstream and downstream primers 0.8 μL, 50 × ROX Reference Dye II 0.4 μL, cDNA 1.0 μL; nuclease-free water was added to 20 μL after the reaction system was configured. The procedures of fluorescence quantitative PCR reaction were: predenaturation (holding stage) at 95 °C 30 s; the cycling stage is at 95 °C 5 s, 55 °C 30 s, 72 °C 30 s, and 40 cycles are carried out in the whole procedures. In addition, each reaction was repeated three times, and the qPCR data were analyzed with the $2^{-\Delta\Delta Ct}$.

2.7. Protein expression detection

The total RNA extract was obtained from colon tissues with the RNAiso Plus reagent. RIPA lysate was added to the samples, and the samples were shaken on the vortex apparatus for 1 min, then stood on ice for 10min, repeated operation 3 times, and the cells were fully lysed, centrifuged at 13,000 rpm at 4 °C for 20 min, and the supernatant of tissue lysate was collected. We determined the protein content via the BCA method. We added a pre-prepared 5 × SDS preloading buffer (EpiZyme, LT101S, China) to the sample and boiled it at 100 °C for 10 min. SDS-PAGE gel was stained with Coomassie brilliant blue. The protein was isolated by SDS-PAGE at a voltage of 160 V and electrophoresis time of 60 min. During SDS-PAGE separation, the loading volume of proteins was set to 60 μg. After electrophoresis, the proteins were soaked in methanol and activated, placed on glue for wet transfer (300 mA constant current, 80–100 min), and then transferred to a PVDF membrane (Amersham, 10600023, Germany). A 5 % skim milk powder sealing solution was prepared with the TBST and sealed for 2 h at room temperature in a shaker. An overnight incubation in a refrigerator at 4 °C was conducted with diluted primary antibodies and sealer solution according to the antibody instructions. All primary antibodies were shown as follows: anti–NF–κB p65 antibody (proteintech, 10745-1-AP); abclonal anti-PCNA antibody (A0264, China); abclonal Antibody for Muc16 (A4666, China); abclonal Antibody against MMP-9 (A11147, China); abclonal antibody for anti-MyD88 (A0980, China); abclonal Antibody for TLR4 (A5258, China); and abclonal antibody for anti-GapDH (A19056, China); Secondary antibodies utilized in this section were abclonal sheep and rat labeled by HRP (AS014, China). After the incubation of the primary antibody, TBST was used to wash the membrane 3 times, 10 min each time. Secondary antibodies were diluted in the sealing solution for incubation at room temperature for 1–2 h. Color development was carried out with a nucleic acid protein gel imager by an enhanced ECL chemiluminescence detection kit (Thermo, 34580, USA) (Bio-Rad, Universal Hood II, USA).

2.8. 16S rRNA sequencing analysis

The 16S rRNA sequencing on our mouse intestinal flora samples was relegated to and completed by Novogene. Our samples were sequenced on the IlluminaNovaSeq platform, and all operations of double-ended sequencing were performed as recommended by the manufacturer. According to the unique barcode of the sample, the pairing end sequence was assigned to the sample, and the barcode and primer sequence introduced by the construction library were removed. A quality filter is applied to the raw read data in QIIME software to remove chimeras and obtain valid sequences. In this sequencing, DADA2 was used for demodulation, and then the concept of ASVs (Amplicon Sequence Variants) was used to construct Operational Taxonomic Units (OUT) tables. The final feature list and feature sequence were obtained for further diversity analysis, species classification annotation, and difference analysis. We normalized diversity and diversity with the same random sequence. With the R studio microbiome package, alpha diversity was used to measure species diversity using the Chao1 index. Wilcoxon rank-sum test was used to examine Shannon indexes and Richness indexes. The diversity indexes showed different patterns among sample groups. With the help of vegan ordinate function, β diversity index was calculated based on OTU (the methods included Constrained principal coordinates analysis (CPCoA)). In the course of distance calculation, the parameters used were Bray-Curtis dissimilarity and weighted UniFrac distance. The other graphs were plotted via R packages.

Table 1
Primer sequences.

Primers	Sequences
PCNA-F	GAACCTCACCAGCATGTCCA
PCNA-R	AATTCACCCGACGGCATCTT
Muc16-F	CAAATGATTGGCCACATTGGA
Muc16-R	CATAGCAGCCAGCTTTGAAGG
MMP-9-F	AACCTCCAACCTCACGGACA
MMP-9-R	TCATCGATCATGTCTCGCGG

3. Results

3.1. Tumor growth in CRC mice is inhibited by Chinese herbal compound

Changes in mouse body weight were shown in Fig. 1A from the beginning to the end of modeling. Over time, the body weight of mice in control group gradually increased, whereas the weight of mice in experimental group increased most rapidly. Model group mice had the slowest body mass growth compared to control group mice. Model mice had significantly shorter colons compared to control mice, and the colon length of mice in the low, medium, and high-dose Chinese herbal compound groups was increased compared with model group (Fig. 1B). The number of colon polyps was significantly increased in the model group, and the number of colon polyps was dose-dependent decreased in low-, medium-, and high-dose Chinese herbal compound groups (Fig. 1C). Immunohistochemistry (IHC) results (Fig. 2A) showed that when compared to model group, Ki-67 protein levels decreased significantly in those treated with medium dose and high dose Chinese herbal compounds. A significant increase in PCNA, Muc16, and MMP-9 protein expression was seen in model group when compared with control group, and the Chinese herbal compound intervention resulted in significant reductions in gene and protein levels (Fig. 2B and C). These results indicated that an herbal compound found in Chinese medicine inhibited the development of colon tumors and the proliferation of colon tissue in mice, and high-dose Chinese herbal compounds produced the best effect.

3.2. Chinese herbal compound relieved CRC mouse colon tissue inflammation along with TLR4/MyD88/NF-κB pathways

According to the results of different doses of Chinese herbal compound intervention in CRC mice tumor formation, the high-dose

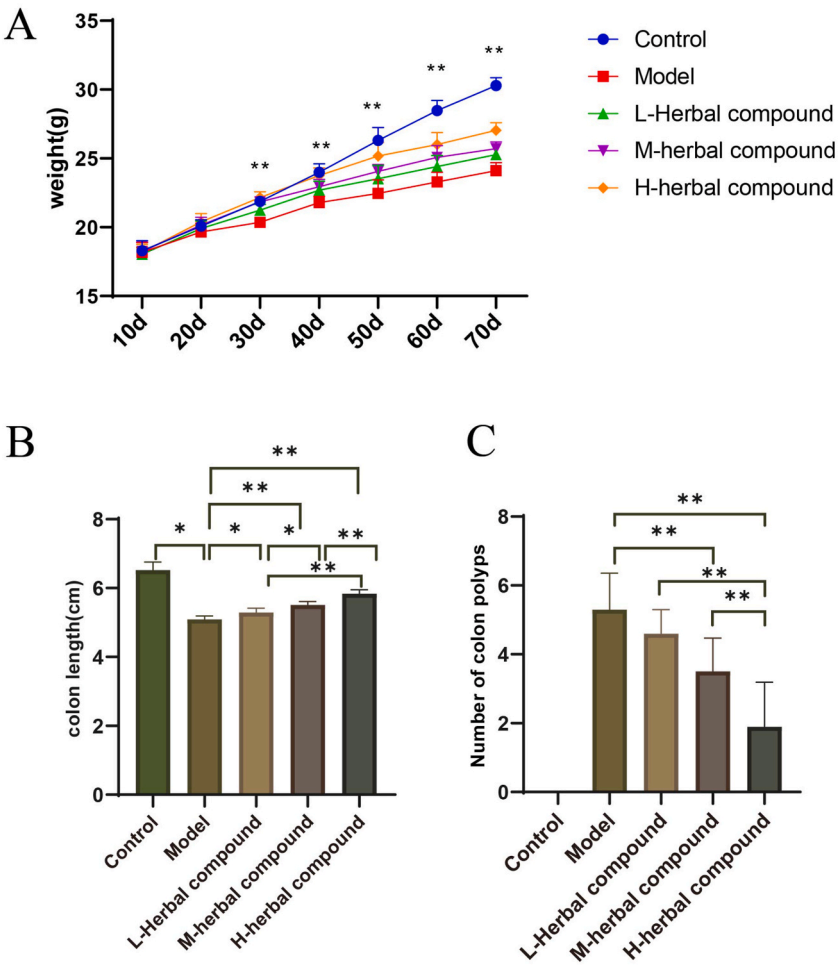

Fig. 1. Incidence of CRC mice tumors and their development in response to Chinese herbal compound. A, Weight changes in CRC mice treated with Chinese herbal compounds at different doses; B, Colon length; and C, The number of polyps in the colon. When the blank control group was taken as reference, *P < 0.05, **P < 0.01; when the model group was deemed as the reference, *P < 0.05, **P < 0.01; when the L-Herbal compound was deemed as the reference, **P < 0.01.

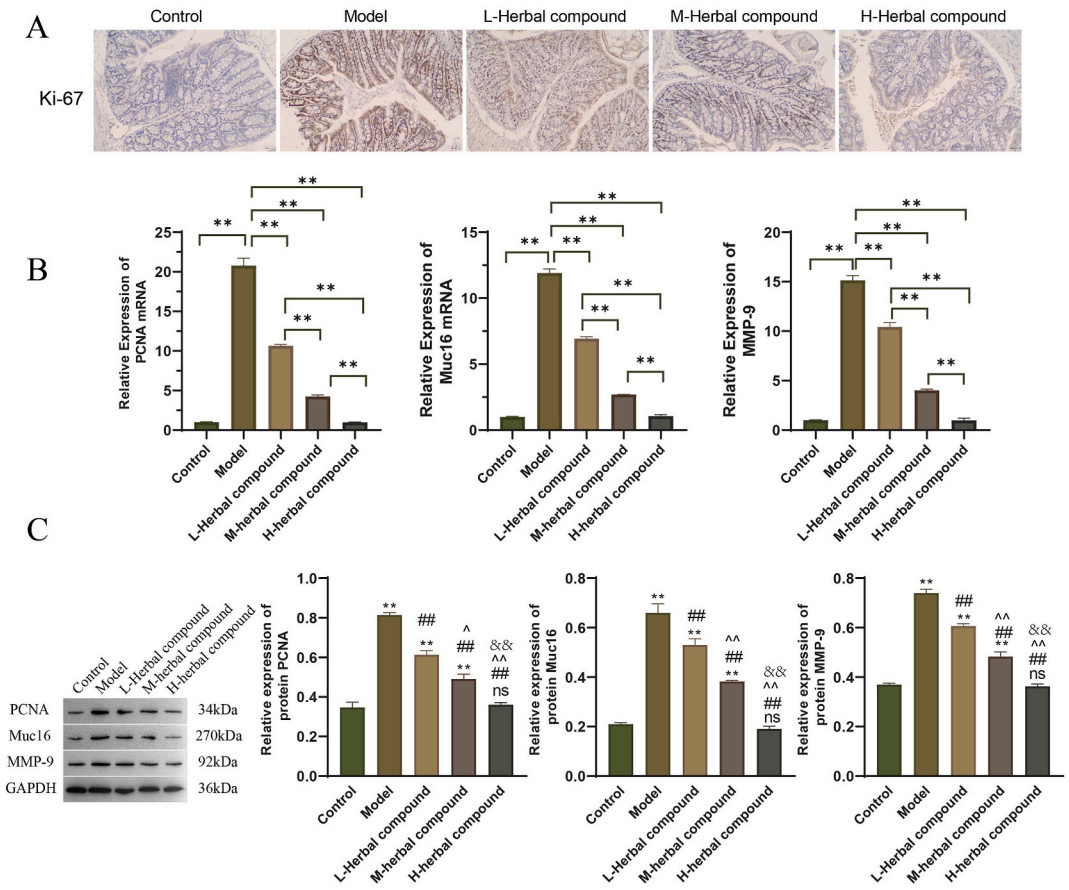

Fig. 2. CRC mice's expression of genes and proteins associated with colon tissue proliferation after Chinese herbal compound treatment. A, Results of immunohistochemistry for Ki-67 in each group (magnification 200, Scale bar = 50 μm); B, mRNA levels of PCNA, Muc16, and MMP-9 in each group; When the blank control group was taken as reference, $^{*}P < 0.05$, $^{**}P < 0.01$; when the model group was deemed as the reference, $^{**}P < 0.01$; when the L-Herbal compound was deemed as the reference, $^{**}P < 0.01$; when the M-Herbal compound was deemed as the reference, $^{**}P < 0.01$. C, Relative expressions of PCNA, Muc16, and MMP-9 proteins in each group. When the blank control group was taken as reference, $^{*}P < 0.05$, $^{**}P < 0.01$; when the model group was deemed as the reference, $\#\#P < 0.01$; when the L-Herbal compound was deemed as the reference, $\hat{}\ P < 0.05$, $\hat{}\hat{}\ P < 0.01$; when the M-Herbal compound was deemed as the reference, && $P < 0.01$.

Chinese herbal compound was chosen as the follow-up study to study the mechanism of CRC drug treatment. The pathological changes of colon tissue of mice in each group were shown in Fig. 3A. Compared to Control group, Model group of mice exhibited loss of intestinal structural integrity, significant tissue damage, and high infiltration of inflammatory cells. However, compared to Model group, Herbal compound group of mice showed higher level of intestinal structural integrity, the destruction of tissue structure and the degree of infiltration of inflammatory cells were reduced.

ELISA results showed that compared to Control group, Model group of mice exhibited elevated levels of IFN-γ, IL-6, and TNF-α in both serum and colon tissue, while IL-10 levels were decreased. In contrast, compared to Model group, Herbal compound group showed decreased levels of IFN-γ, IL-6, and TNF-α in both serum and colon tissue, while IL-10 levels were increased (Fig. 3B and C).

Fig. 4A, B showed the relative expression of TLR4, MyD88, and NF-κB p65 mRNA in the colon tissue of mice. Expressions of TLR4, MyD88, and NF-κB p65 in normal group and model group were significantly increased, and after medication administration, mice showed significantly decreased mRNA and protein levels of TLR4, MyD88, and NF-κB p65.

3.3. Intestinal flora composition analysis on mice treated with Chinese herbal compound

The stool samples from both mouse groups were sequenced. A default unit of OTUs was taken on account of the clustering results of OTUs with 97 % similarity, and our Venn diagrams illustrated the number of common and different OTUs between groups. The number of OTUs in control group, model group, and administration group was 179, 174, and 189 respectively, and the intersection number of the three groups was 78.

The results showed (Fig. 5A) that a decrease in OTUs was seen in model group, while an increase in OUTs was seen in administration group, suggesting that there may be an increase in flora richness as a result of Chinese herbal compound intervention. As shown

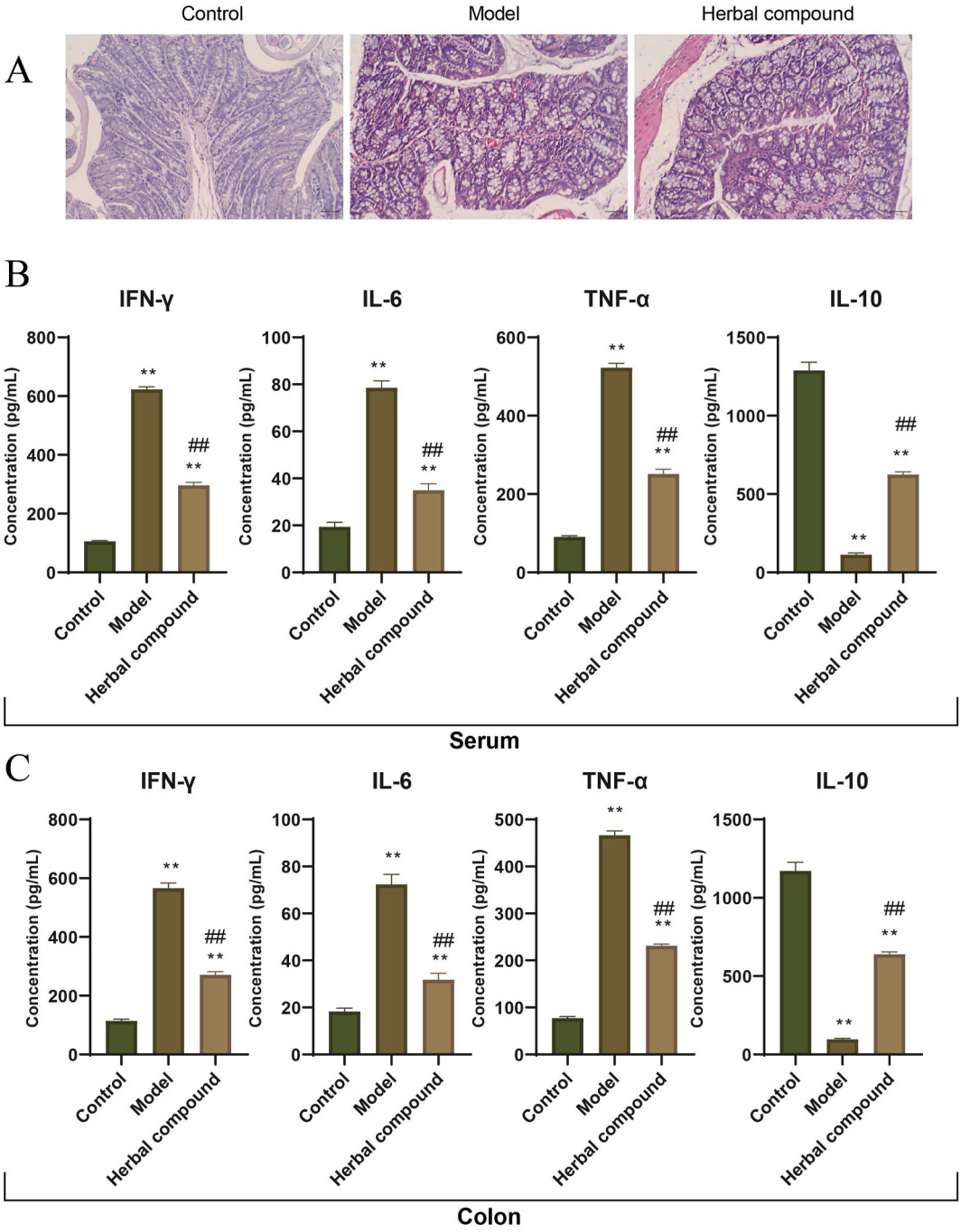

Fig. 3. Consequence of Chinese herbal compounds on colon tissue inflammation in CRC mice. A, Each group's colonic histopathology was assessed through HE staining (magnification 200, Scale bar = 50 μm); B, Serum levels of IL-6, TNF-α, IFN-γ, and IL-10 were detected by ELISA; C, The levels of IL-6, TNF-α, IFN-γ and IL-10 in colon tissue of mice were determined by ELISA. When the blank control group was taken as a reference, $*P < 0.05$, $**P < 0.01$; when the model group was deemed as a reference, $\#\#P < 0.01$.

in Fig. 5B, the intestinal flora was further subjected to analyses in aspects of phylum, class, order, and family. As compared to the dominant bacteria in the control group, Bacteroidales_S24-7_group in model group and administration group decreased; there was a reduction in Lachnopiraceae in the administration group, whereas it dominated in the model group.

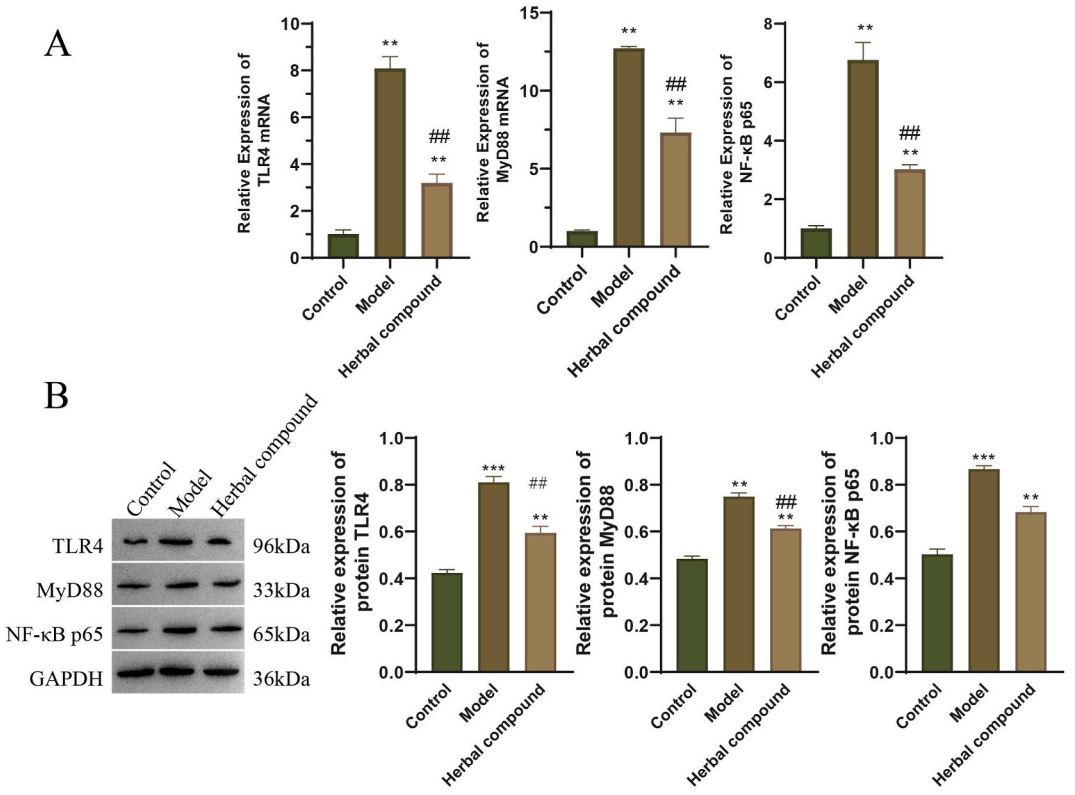

Fig. 4. Expression of TLR4/MyD88/NF-κB pathway protein in mice of each group. A, Expression of TLR4, MyD88, NF-κB p65 mRNA in mice; B, Expression of TLR4, MyD88, and NF-κB p65 in mice. When a blank control group was taken as reference, $*P < 0.05$, $**P < 0.01$; when the model group was used as a reference, $\#\#P < 0.01$.

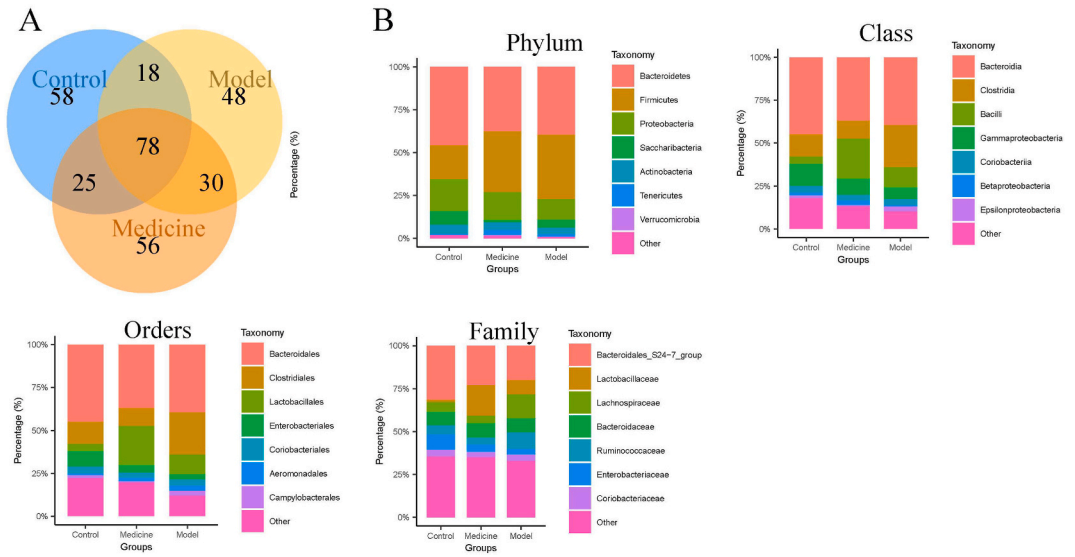

Fig. 5. The analysis of the relative abundance of intestinal microorganisms within each group. A, Different groups of Venn diagrams were drawn with OTUs as the unit; B, Relative abundance of intestinal microorganisms on Phylum, Class, Orders, and Family levels in each group.

3.4. Comparison of the microbial diversity of intestinal flora and its markers in different groups of mice

The Alpha diversity measures the number of microbes in a single sample and the proportion of each species, focusing on the richness and evenness of the sample's flora. Alpha diversity analysis of intestinal flora in the control group, model group, and administration group was shown in Fig. 6A: the Richness indexes and Chao1 indexes in the model group were decreased, which suggested that the species Richness changes were not statistically significant. The Chao1 indexes and richness indexes in the administration group were increased compared with the model group. The CPCoA diagram showed that there was a clustering of samples from the control and model groups closer together and clustered into one, while the samples from the administration group were scattered (Fig. 6B). Fig. 6C shows a temperature map of the distance matrices of Beta diversity. An analysis of LEfSe data was conducted to identify the characteristics of the abundance of different species between groups and their associated classes. Control, model, and administration groups were compared via LEfSe to assess the differences in intestinal microbes. As shown in Fig. 7A and **B**, the relative abundance of Lactobacillaceae, Lactobacillales, Aeromonadaceae, etc. in model group and control group was significantly different.

3.5. Prediction of tertiary metabolic pathways of different groups of mice

As shown in Fig. 8A and B, there were significant differences in the relative abundance of amino acid metabolism between control group and model group; besides, a significant difference was observed between control group and model group in beta-alanine metabolism, tryptophan metabolism, glycine serine, and threonine metabolism. Fig. 8C showed that administration group had significantly lower abundances of the transcription machinery, carbon fixation in photosynthetic organisms, and valine leucine and isoleucine biosynthesis than model group.

4. Discussion

Despite being one of the most common malignant tumors, large intestine cancer has a complex pathogenesis, and the existing clinical evidence shows that the pathogenesis is relevant to the abnormality of numerous signaling pathways [27–30]. TCM components are complex and diverse, some of which simultaneously inhibit the growth of pathogenic bacteria and promote the colonization of probiotics. While activating the anti-inflammatory effect of intestinal immune cells, they also reduce the permeability of intestinal

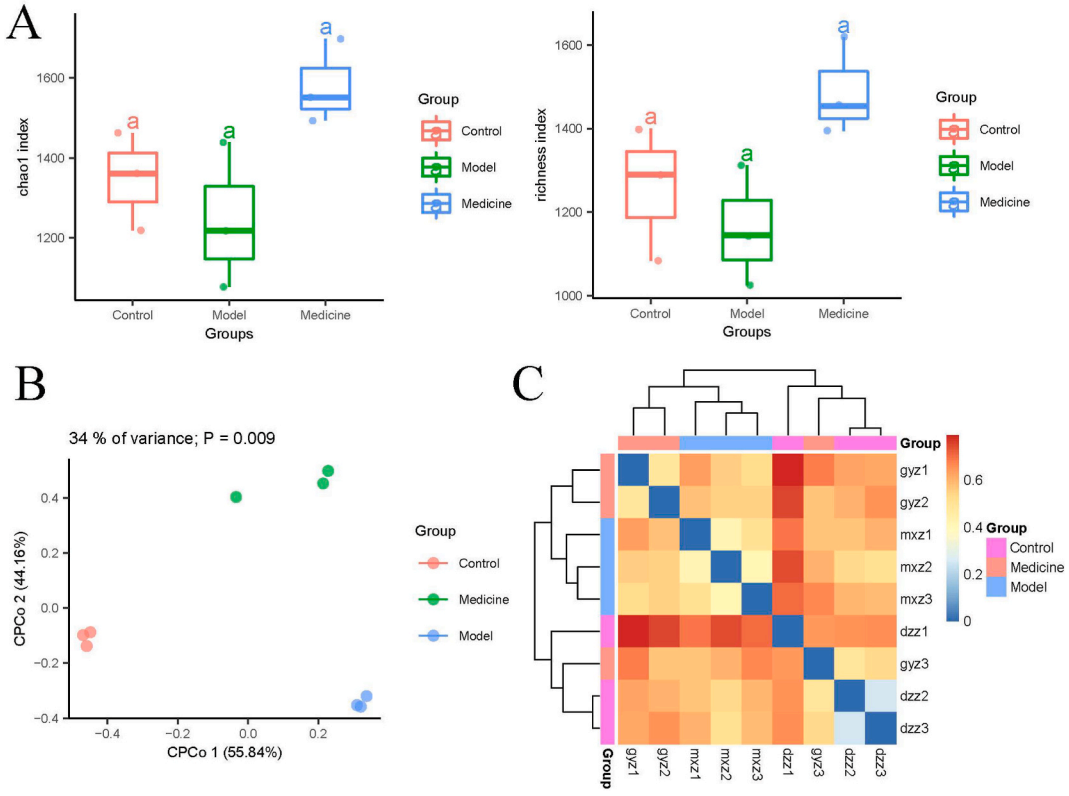

Fig. 6. Heterogeneity of intestinal microbial community. A, OTU-based alpha diversity (Chao1 index and Richness index); B, Weighted-Unifrac-distance-based restrictive principal coordinate analysis; C, Bray-curits distance matrix heat map.

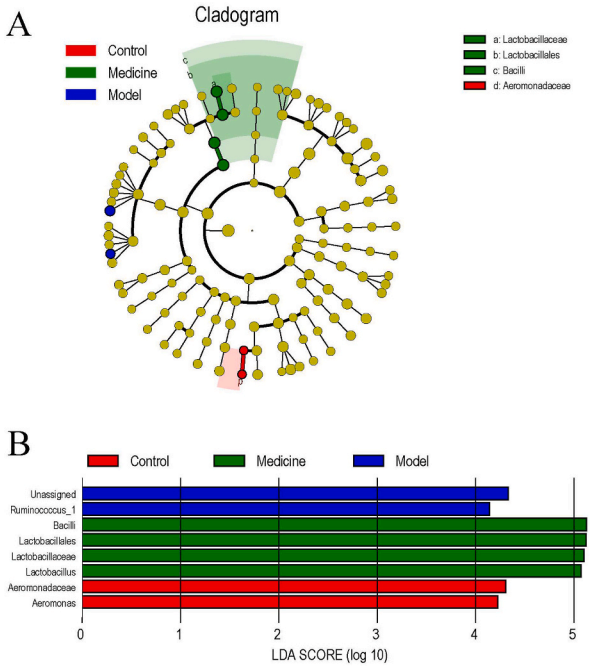

Fig. 7. Species with significant inter-group differences identified by linear discriminant analysis effects. A. Tree diagram of LEfSe analysis; B, LEfSe analysis bar chart.

mucosa and prevent the invasion of pathogenic bacteria, thus maintaining the stability of intestinal microecology. Through in vivo experiments in mice, this study investigated the effects of Chinese herbal compounds on large intestine cancer tumor development and intestinal flora. The theoretical basis of this study was to study the mechanism of Chinese herbal compounds in the treatment of large intestine cancer based on the TLR4/MyD88/NF-κB pathway, to explore the effects on intestinal flora composition and metabolic pathway differences. Our results showed that low-, medium- and high-doses of Chinese herbal compound increased colon length and reduced the number of colon polyps in the model group, which also resulted in the inhibition of the relative expression of genes and proteins relevant to colon tissue proliferation (PCNA, Muc16, MMP-9). In addition, we found that the Chinese herbal compound in high-dose group also had the function of reducing IL-6, TNF-α, and IFN-γ inflammatory factors in serum and colon tissue, inhibiting the destruction of tissue structure and alleviating the degree of inflammatory cell infiltration. The effect of the Chinese herbal compounds on the expression level of TLR4/MyD88/NF-κB was verified by experiments. It also suggested that the Chinese herbal compound treatment CRC was regulated by TLR4/MyD88/NF-κB signaling pathway. Subsequently, the 16S rRNA sequencing experiment was performed to determine the differences in intestinal flora composition and metabolic pathways among the model, Chinese herbal compound treatment, and control groups. Our results showed that the flora abundance varied significantly between control group and model group, and the flora diversity showed a decrease in model group, while the relative abundance of amino acid metabolism was significantly different between control group and model group.

Patients with colorectal cancer are usually treated with a combination of surgery, chemotherapy and radiation. However, a multitude of patients still suffer a high recurrence rate and the risk of distant metastasis remains [31,32]. Although chemotherapy is an important means to consolidate curative effects and prevent recurrence and metastasis in the treatment of CRC, it might cause liver and kidney function injury, neurotoxic adverse reactions, and gastrointestinal dysfunction. Clinical practices have demonstrated the effectiveness of TCM treatment in inhibiting tumor metastasis and recurrence, and its supportive role in postoperative chemotherapy for CRC [16,33]. This Chinese herbal compound consists of *Hedyotis diffusa Willd, Scutellaria barbata D.Don, and Radix Astragali*, known for their functions in heat-clearing, detoxification, enriching blood qi, and promoting digestion [34,35]. In herbal formulation, *Hedyotis diffusa Willd* is cold in nature, sweet and bitter in flavor, and nontoxic [36,37]. It primarily affects the stomach, large intestine, and small intestine meridians, providing functions such as clearing heat, detoxifying, treating carbuncles, promoting blood circulation, and relieving pain [38]. *Scutellaria barbata D.Don* medicine trait is pungent, bitter, and cold. Its efficacy mainly acts on the lung, liver, kidney, and large intestine, and it can clear heat and detoxify, promote blood circulation and remove blood stasis, reduce swelling, and relieve pain [38,39]. *Hedyotis diffusa Willd* and *Scutellaria barbata D.Don*, when used in combination as a medicinal pair, exhibited anti-tumor effects. These effects included inducing tumor cell apoptosis, inhibiting tumor cell proliferation, enhancing immune responses, and reducing telomerase activity [40]. According to the previous studies, Te-Hsin Chao et al. discovered that *Hedyotis diffusa Willd* and *Scutellaria barbata D.Don* are anti-inflammatory and antioxidant, thus being anti-tumor [41]. In this study, we found that the Chinese herbal compound could inhibit the shortening of colon length and reduce the number of colon polyps, and the positive expression of Ki-67 in colon tissues decreased. After Chinese herbal compound intervention, PCNA, Muc16, and MMP-9 gene expression decreased significantly. PCNA is closely related to cell DNA synthesis, involving the initiation of cell proliferation, and it is a

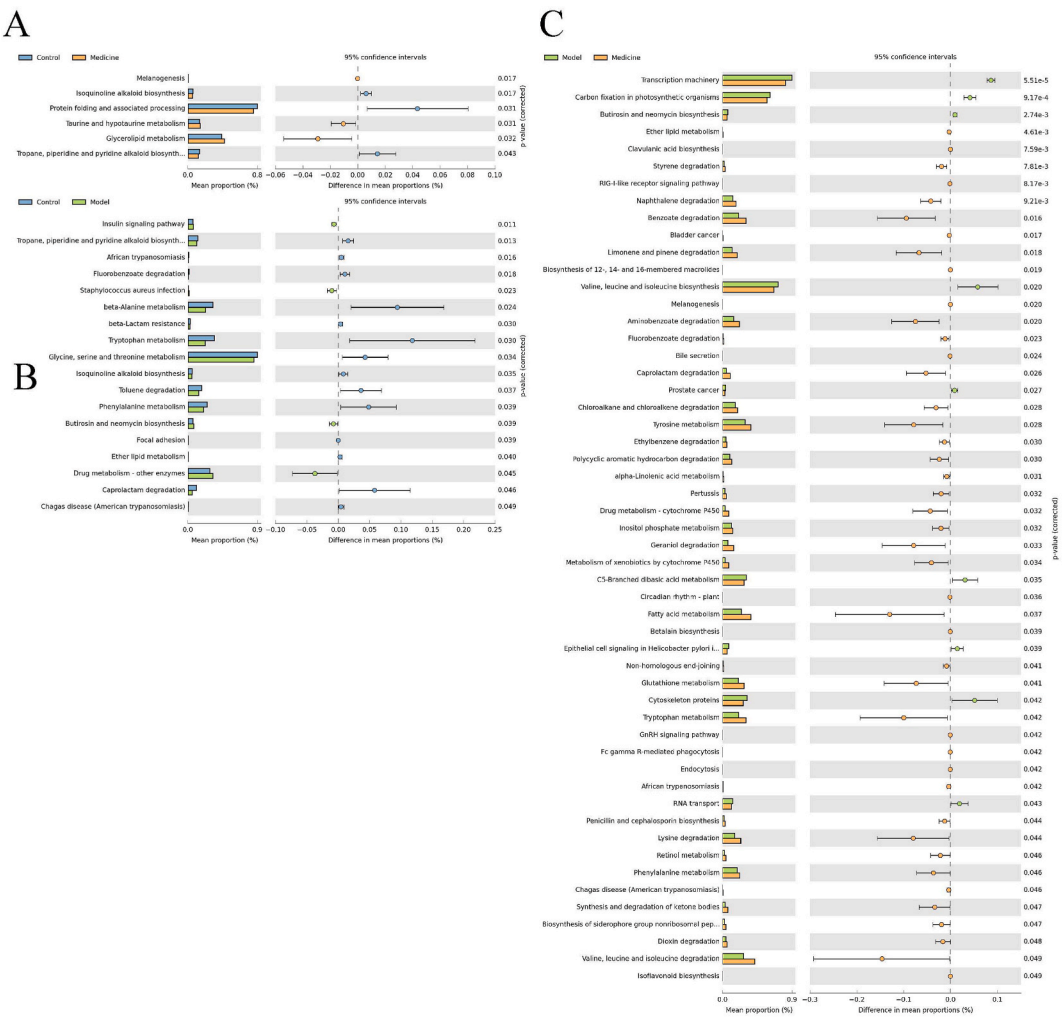

Fig. 8. The Layer 3 classification metabolic pathway analysis onto the difference amid control group, model group, and administration group. A, The Layer 3 classification metabolic pathway analysis to the difference between the control group and administration group; B, The Layer 3 classification metabolic pathway analysis to the difference between the control group and model group; C, The Layer 3 classification metabolic pathway analysis to the differences amid model group and administration group. Different color bars represented different groups. The bar chart listed the level 3 classification of KEGG metabolic pathways with significant differences within groups in the level 3 composition and their proportions in each group. In addition, the ratio and confidence interval of difference and *P*-value were given on the right. (For interpretation of the references to color in this figure legend, the reader is referred to the Web version of this article.)

good indicator reflecting cell proliferation status. CRC is associated with the PCNA index, which has been considered an independent prognostic factor [42]. Additionally, the expression of PCNA and Ki-67 in CRC may indicate the development of lymph node metastasis [43]. There has been widespread use of the biomarker MUC16 (formerly known as CA125) in ovarian cancer diagnosis; apart from ovaries [44], abnormal over-expression of this gene has also been observed in pancreas [45], breast [46], and colon cancers [47]. This suggests that high expression of MUC16 is associated with cancer progression, metastasis, and poor prognosis in patients [48]. There are several factors contributing to the occurrence and development of CRC, including inflammatory factors and MMP.

Intestinal flora is an important part of the intestine and warrants specific attention for the reason that it can induce intestinal inflammation and damage the intestinal barrier through various mechanisms, affecting the occurrence and development of CRC. Changes in the composition of intestinal flora will lead to inflammation and even cancer caused by some strains in the intestine, which is a factor that has a substantial impact on the occurrence and development of CRC [49]. CRC is believed to be caused by an imbalance in the intestinal flora, mainly via the following mechanisms: the imbalance of intestinal flora leads to increased permeability of intestinal mucosa; the aggravation of intestinal mucosal epithelial damage due to abnormal pro-inflammatory response signals; the toxic metabolites of certain intestinal microorganisms lead to intestinal epithelial cells [50]. There has been significant evidence that CRC patients have altered intestinal flora. Besides, there is also a significant difference between the dominant flora and the diversity of intestinal flora in patients with large intestine cancer in their feces [17]. We harnessed a high-dose Chinese herbal compound to intervene in the CRC model mice and detected the changes in inflammatory factors in the mice. The results showed that the colon

tissues of CRC mice showed obvious inflammatory infiltration, the levels of inflammatory factors in serum and colon tissues increased significantly, and the inflammatory conditions of CRC mice were inhibited after high-dose Chinese herbal compound intervention. Furthermore, mice stool samples were collected for 16S rRNA analysis, which correlated well with the research. Our study also showed that a significant reduction in Bacteroidales abundance was observed in CRC mice compared with normal mice in terms of intestinal flora diversity. In addition, our research also has the following findings: first, the TLR4/MyD88/NF-κB pathway is involved in regulating colon cancer progression; secondly, the imbalance in the intestinal flora may contribute to cancer by inducing abnormal inflammatory response and altering the local immune microenvironment of the colon, and inflammation may be related to the progression of CRC [51].

However, this study also has the following limitations: firstly, the effects of Chinese herbal compounds on colon cancer proliferation and inflammation were only studied in mice, which lacked verification at the cellular level; secondly, the sample size of 16S rRNA analysis is too small, resulting in inaccurate data analysis results.

5. Conclusion

Taken together, CRC mice treated with Chinese herbal compound showed a reduced inflammatory response and suppressive cancer progression; high-dose Chinese herbal compound had the optimal efficiency, and the underlying mechanism for CRC treatment might be its involvement in the TLR4/MyD88/NF-κB pathway regulation. Further, the microflora diversity of CRC mice decreased, and the dominant microflora was significantly different between CRC mice and normal mice. Bacteroidales abundance was substantially decreased in CRC mice as compared with the Control.

Data availability statement

All of the result data supporting this study are included within the article.

Funding

This study was supported by the Project of Chongqing Science and Technology Bureau, China (No.cstc2019jxj1130013), the Chongqing Science and Health Joint Medical Research Project(2022ZDXM036), and Special Project for Performance Incentive and Guidance of Scientific Research Institutions in Chongqing (cstc2021jxjl130020).

CRediT authorship contribution statement

Pingyu Liu: Methodology, Formal analysis, Conceptualization. **Jian Ying:** Conceptualization, Writing - original draft. **Xin Guo:** Writing - review & editing, Writing - original draft, Methodology, Conceptualization. **Xiaohui Tang:** Software, Formal analysis. **Wenjuan Zou:** Supervision, Methodology, Data curation. **Tiantian Wang:** Visualization, Supervision, Methodology. **Xinyi Xu:** Methodology, Software. **Bin Zhao:** Investigation, Supervision. **Na Song:** Methodology, Investigation. **Jun Cheng:** Writing - review & editing, Writing - original draft, Resources, Conceptualization.

Declaration of competing interest

The authors declare that they have no known competing financial interests or personal relationships that could have appeared to influence the work reported in this paper.

Appendix A. Supplementary data

Supplementary data to this article can be found online at https://doi.org/10.1016/j.heliyon.2023.e23533.

References

[1] H. Sung, et al., Global cancer statistics 2020: GLOBOCAN estimates of incidence and mortality worldwide for 36 cancers in 185 countries, CA Cancer J Clin 71 (3) (2021) 209–249.
[2] L. Zongchao, et al., Interpretation on the report of global cancer statistics 2020, Electronic Journal of Integrative Oncology Therapy 7 (2) (2021) 1–14.
[3] J. Li, et al., Integrating network pharmacology and experimental validation to explore the effect and mechanism of AD-1 in the treatment of colorectal cancer, Front. Pharmacol. 14 (2023), 1159712.
[4] S. Huang, et al., Kangai Injection, a Traditional Chinese Medicine, Improves Efficacy and Reduces Toxicity of Chemotherapy in Advanced Colorectal Cancer Patients: A Systematic Review and Meta-Analysis vol. 2019, Evid Based Complement Alternat Med, 2019, 8423037.
[5] J. Du, et al., Assessment of the targeted effect of Sijunzi decoction on the colorectal cancer microenvironment via the ESTIMATE algorithm, PLoS One 17 (3) (2022), e0264720.
[6] Q. Meng, et al., Epstein-barr virus-encoded MicroRNA-BART18-3p promotes colorectal cancer progression by targeting de novo lipogenesis, Adv. Sci. 9 (35) (2022), e2202116.
[7] S. Han, et al., Progress in research on colorectal cancer-related microorganisms and metabolites, Cancer Manag. Res. 12 (2020) 8703–8720.

[8] F. Zarghampoor, B. Valibeigi, A. Behzad-Behbahani, The molecular characteristics of colorectal cancer: impact of Ibuprofen and hyperthermia, Mol. Biol. Res. Commun. 12 (1) (2023) 17–25.
[9] M. Zhong, et al., TIPE regulates VEGFR2 expression and promotes angiogenesis in colorectal cancer, Int. J. Biol. Sci. 16 (2) (2020) 272–283.
[10] M. Hu, et al., Identification of differently expressed genes associated with prognosis and growth in colon adenocarcinoma based on integrated bioinformatics analysis, Front. Genet. 10 (2019) 1245.
[11] J. Zhang, et al., Research progress of traditional Chinese medicine in the adjuvant treatment of colorectal cancer, Chinese Medicine Modern Distance Education of China 19 (7) (2021) 3.
[12] M. McCulloch, et al., Colon cancer survival with herbal medicine and vitamins combined with standard therapy in a whole-systems approach: ten-year follow-up data analyzed with marginal structural models and propensity score methods, Integr. Cancer Ther. 10 (3) (2011) 240–259.
[13] Y.T. Liu, et al., Traditional Chinese medicine formula T33 inhibits the proliferation of human colorectal cancer cells by inducing autophagy, Environ. Toxicol. 37 (5) (2022) 1007–1017.
[14] Y. Chen, et al., Proteome analysis of camellia nitidissima chi revealed its role in colon cancer through the apoptosis and ferroptosis pathway, Front. Oncol. 11 (2021), 727130.
[15] X. Kong, et al., Combination of UPLC-Q-TOF/MS and network pharmacology to reveal the mechanism of qizhen decoction in the treatment of colon cancer, ACS Omega 6 (22) (2021) 14341–14360.
[16] W. Peng, et al., Jianpi Jiedu decoction, a traditional Chinese medicine formula, inhibits tumorigenesis, metastasis, and angiogenesis through the mTOR/HIF-1α/VEGF pathway, J. Ethnopharmacol. 224 (2018) 140–148.
[17] Y. Cheng, Z. Ling, L. Li, The intestinal microbiota and colorectal cancer, Front. Immunol. 11 (2020), 615056.
[18] C.V. De Almeida, et al., Role of diet and gut microbiota on colorectal cancer immunomodulation, World J. Gastroenterol. 25 (2) (2019) 151–162.
[19] Y. Fang, et al., The roles of microbial products in the development of colorectal cancer: a review, Bioengineered 12 (1) (2021) 720–735.
[20] Z. Liu, et al., A review on the immunomodulatory mechanism of acupuncture in the treatment of inflammatory bowel disease, Evid Based Complement Alternat Med 2022 (2022), 8528938.
[21] T. Wan, et al., NLRP3-Dependent pyroptosis: a candidate therapeutic target for depression, Front. Cell. Neurosci. 16 (2022), 863426.
[22] B. Zhang, et al., DL0410 alleviates memory impairment in D-galactose-induced aging rats by suppressing neuroinflammation via the TLR4/MyD88/NF-κB pathway, Oxid. Med. Cell. Longev. 2021 (2021), 6521146.
[23] T. Saito, et al., Importance of endothelial NF-κB signalling in vascular remodelling and aortic aneurysm formation, Cardiovasc. Res. 97 (1) (2013) 106–114.
[24] F. Long, et al., Atractylenolide-I suppresses tumorigenesis of breast cancer by inhibiting toll-like receptor 4-mediated nuclear factor-κb signaling pathway, Front. Pharmacol. 11 (2020), 598939.
[25] K. Bi, et al., MicroRNAs regulate intestinal immunity and gut microbiota for gastrointestinal health: a comprehensive review, Genes 11 (9) (2020).
[26] X. Sun, et al., Alantolactone inhibits cervical cancer progression by downregulating BMI1, Sci. Rep. 11 (1) (2021) 9251.
[27] L.F.S. Oliveira, et al., Therapeutic potential of naturally occurring small molecules to target the wnt/β-catenin signaling pathway in colorectal cancer, Cancers 14 (2) (2022).
[28] N. Wei, et al., The cytotoxic effects of regorafenib in combination with protein kinase D inhibition in human colorectal cancer cells, Oncotarget 6 (7) (2015) 4745–4756.
[29] A.K. Chow, et al., Preclinical analysis of the anti-tumor and anti-metastatic effects of Raf265 on colon cancer cells and CD26(+) cancer stem cells in colorectal carcinoma, Mol. Cancer 14 (2015) 80.
[30] K. Hou, et al., Microbiota in health and diseases, Signal Transduct Target Ther 7 (1) (2022) 135.
[31] D.H. Chen, et al., Non-coding RNA m6A modification in cancer: mechanisms and therapeutic targets, Front. Cell Dev. Biol. 9 (2021), 778582.
[32] Y.Y. Wu, et al., Mean platelet volume/platelet count ratio in colorectal cancer: a retrospective clinical study, BMC Cancer 19 (1) (2019) 314.
[33] L. Zhao, et al., Xiaoyaosan, a traditional Chinese medicine, inhibits the chronic restraint stress-induced liver metastasis of colon cancer in vivo, Pharm. Biol. 58 (1) (2020) 1085–1091.
[34] H. Wu, et al., Clinical efficacy of modified yiwei shengyang decoction combined with FOLFOX4 chemotherapy regimen in the treatment of advanced gastric cancer and its effect on tumor marker levels, Evid Based Complement Alternat Med 2022 (2022), 6234032.
[35] L. Gao, et al., Clinical effects of Chinese herbal decoction combined with basic chemoradiotherapy and nursing intervention in the treatment of cervical cancer and the effect on serum CEA, CA125, and TNF-α levels, Evid Based Complement Alternat Med 2021 (2021), 1446864.
[36] D. Zhang, et al., [Regularity of prescriptions for intermediate and advanced lung cancer based on latent structure combined with association rules], Zhongguo Zhongyao Zazhi 47 (1) (2022) 235–243.
[37] Z. Chen, et al., Development of models for classification of action between heat-clearing herbs and blood-activating stasis-resolving herbs based on theory of traditional Chinese medicine, Chin. Med. 13 (2018) 12.
[38] Y. Shen, et al., The pharmacological mechanism of the effect of plant extract compound drugs on cancer pain based on network pharmacology, J Healthc Eng 2022 (2022), 9326373.
[39] C. Huang, et al., AURKB, CHEK1 and NEK2 as the potential target proteins of Scutellaria barbata on hepatocellular carcinoma: an integrated bioinformatics analysis, Int. J. Gen. Med. 14 (2021) 3295–3312.
[40] Y. Hui, L. Qingtao, The progress of the anti-tumor activity of Oldenlandia diffusa,Scutellaria barbara and their combination, Journal of Modern Oncology 23 (22) (2015) 3353–3356.
[41] T.H. Chao, et al., Prescription patterns of Chinese herbal products for post-surgery colon cancer patients in Taiwan, J. Ethnopharmacol. 155 (1) (2014) 702–708.
[42] D. Kovac, et al., Proliferating cell nuclear antigen (PCNA) as a prognostic factor for colorectal cancer, Anticancer Res. 15 (5b) (1995) 2301–2302.
[43] K. Guzińska-Ustymowicz, et al., Correlation between proliferation markers: PCNA, Ki-67, MCM-2 and antiapoptotic protein Bcl-2 in colorectal cancer, Anticancer Res. 29 (8) (2009) 3049–3052.
[44] A. Aithal, et al., MUC16 as a novel target for cancer therapy, Expert Opin. Ther. Targets 22 (8) (2018) 675–686.
[45] D. Thomas, et al., Isoforms of MUC16 activate oncogenic signaling through EGF receptors to enhance the progression of pancreatic cancer, Mol. Ther. 29 (4) (2021) 1557–1571.
[46] I. Lakshmanan, et al., MUC16 induced rapid G2/M transition via interactions with JAK2 for increased proliferation and anti-apoptosis in breast cancer cells, Oncogene 31 (7) (2012) 805–817.
[47] Z. Liu, et al., Mucin 16 promotes colorectal cancer development and progression through activation of janus kinase 2, Dig. Dis. Sci. 67 (6) (2022) 2195–2208.
[48] D. Gupta, C.G. Lis, Role of CA125 in predicting ovarian cancer survival - a review of the epidemiological literature, J. Ovarian Res. 2 (2009) 13.
[49] M. Chen-xue, et al., Advances in intestinal flora stability and colorectal cancer, J. Microbiol. 40 (2) (2022) 108–114.
[50] X. Zhou, et al., Effect and mechanism of vitamin D on the development of colorectal cancer based on intestinal flora disorder, J. Gastroenterol. Hepatol. 35 (6) (2020) 1023–1031.
[51] Q. Li, et al., The effects of cellulose on AOM/DSS-Treated C57bl/6 colorectal cancer mice by changing intestinal flora composition and inflammatory factors, Nutr. Cancer 73 (3) (2021) 502–513.